Dynamic modelling of local low-temperature heating grids: a case study for Norway

Hanne Kauko[a,*], Karoline Husevåg Kvalsvik[a], Daniel Rohde[b], Armin Hafner[b], Natasa Nord[b]

[a]*SINTEF Energy Research, Kolbjørn Hejes vei 1B, Trondheim 7491, Norway*
[b]*Department of Energy and Process Engineering, Norwegian University of Science and Technology (NTNU), Kolbjørn Hejes vei 1B, Trondheim 7491, Norway*

Abstract

Today's district heating (DH) networks in Norway are 2nd and 3rd generation systems, with supply temperatures ranging from 80-120 °C. In new developments, it is desirable to shift to 4th generation, low-temperature district heating (LTHD) in order to reduce the heat losses and enable better utilization of renewable and waste heat sources. A local LTDH grid for a new development planned in Trondheim, Norway, has been modelled in the dynamic simulation program Dymola in order to study the effect of lowered supply temperatures to heat losses and circulation pump energy use. Different cases with supply temperatures ranging from 55 to 95 °C, lowered return temperature as well as peak shaving were analyzed. Real DH use data for buildings in Trondheim were employed. The environmental impact in terms of the total produced CO_2 equivalent emissions was estimated for each case, assuming a heat production mix corresponding to that of the local DH provider. The results showed that by lowering the supply temperature to 55°C, the heat losses could be reduced by one third. The total pump energy increased significantly with reduced supply temperature, however the pump energy was generally an order of magnitude lower than the heat losses.

Keywords: Low-temperature district heating, Thermal system modelling, Energy planning

1. Introduction

District heating (DH) will play an important role in the future fossil-free energy systems by allowing an increased utilization of renewable heat and waste heat sources, however, a prerequisite for this is a reduction in the distribution temperatures [1, 2]. Through reduced supply temperature, DH production with renewable heat sources, such as solar thermal and heat pumps, becomes more efficient. Utilization of heat pumps in DH production becomes more beneficial with reduced supply temperatures as it enables improved coefficient of performance (COP) for the heat pumps, resulting into lower heat costs and primary energy use [3]. Reduced temperature level allows also improved utilization of low-temperature waste heat sources from buildings and industry [2]. Moreover, the distribution heat losses will be greatly reduced with lowered distribution temperatures [4, 5], and shifting to cheaper piping materials is enabled [2].

Current DH networks in Norway are 2nd and 3rd generation systems, with supply temperatures ranging from 80 to 120 °C. The DH companies are nevertheless interested in lowering the temperature level to comply with the lower heat demand of modern building mass, as well as to reduce heat losses. In Denmark, low-temperature DH (LTDH) systems with supply temperatures down to 50-55 °C have already been introduced [6]. In Norway, however, the minimum temperature requirement is limited to 65 °C by legislation related to control of Legionella [7], whenever domestic hot water (DHW) preparation is required. This is still a considerable reduction considering today's temperature levels.

Due to the high investment costs related to DH systems, there is a great interest in simulation and planning software to find the most optimal solutions regarding production and distribution of heat [8]. There are many software tools available for simulation of DH systems; a comprehensive overview has been given in [9]. Optimization with respect

*Corresponding author
Email address: hanne.kauko@sintef.no (Hanne Kauko)

Table 1: The modelled building stock.

Building type	Number	Area [m^2]	Share
Apartment block	18	140 898	75 %
Nursery	3	4 400	2 %
School	1	6 000	3 %
Nursing home	1	12 600	7 %
Culture building	1	4 000	2 %
Sports hall	1	10 000	5 %
Main building	1	5 850	3 %
Psychiatric hospital	1	3 700	2 %
Other historical buildings	1	300	0.2 %
Total	28	185 748	100 %

to e.g. energy efficiency or exergy, costs and environmental impact is usually the main objective for such software [9]. For detailed physical modelling of DH systems, the dynamic simulation program Dymola using the object-oriented modelling language Modelica has been proven to be a flexible and efficient tool [5, 8, 10, 11].

In the present study, the potential of LTDH for a green neighborhood, Brøset, planned in Trondheim, Norway, has been investigated using Dymola/Modelica. The total heat demand, heat losses and the energy demand of the circulation pump were analyzed for three different supply temperatures: 95 °C with outdoor temperature compensation, and constant supply temperatures of 65 and 55 °C. In addition, the effect of lowered return temperature and peak shaving were analyzed. In order to have realistic demand profiles, the DH demand of the building mass was modelled using real DH use data for buildings from the same region.

The objectives of this study were to perform a quantitative assessment of DH grid performance in terms of thermal and hydraulic losses in modern building areas; to demonstrate the potential savings in energy and greenhouse gas (GHG) emissions enabled through lowered distribution temperatures; as well as to validate the use of Dymola as a tool for modelling local heating grids. The central research questions are: (1) What is the impact of lowered supply temperatures on heat losses and pump energy use and (2) How do lowered distribution temperatures affect the DH-related GHG emissions for the case of Trondheim.

2. Methodology

The methodology consisted of three primary steps:

1. Collect data for DH demand profiles for modern buildings representing different building categories, located in Trondheim (results presented in a separate report [12]). Select suitable demand profiles to represent the building stock at Brøset.
2. Create a model in Dymola for the local heating network, including the buildings, piping network and a heat supply plant.
3. Simulate different scenarios with various supply temperature levels in order to study the feasibility of a LTDH network from an energetic and environmental perspective.

These phases will be described in more detail in the following.

2.1. The building stock

The investigated building area was a new neighborhood, Brøset, which is planned to be built in Trondheim, Norway. The building types, number of buildings in each category and the total building area are given in Table 1. The area was of interested because the local DH company will have to provide a solution for heat supply for this area in the future. Furthermore, the area will include several types of buildings as shown in Table 1, and it was interesting to analyze the heat supply system for an area with such a heterogeneous building stock. Several protected historical buildings are present in the area as well (main building, psychiatric hospital and another smaller building, see Table 1). The total area of the neighborhood was 344 000 m^2.

The DH demand of the buildings was modelled using real DH use data from existing buildings, with the building type and standard matching with the buildings to be built as well as possible. For apartment blocks for instance, DH use data from apartment blocks built according to the Norwegian passive house standard were used [13], as this is the newest building standard and is on its way to become the national building code. The data included the total heating demand, i.e., both space heating and DHW preparation. The duration curves for each building type are shown in Figure 1. The motivation to use existing data was to be able to model the simultaneity of heat demand peaks throughout a day and the year as realistically as possible.

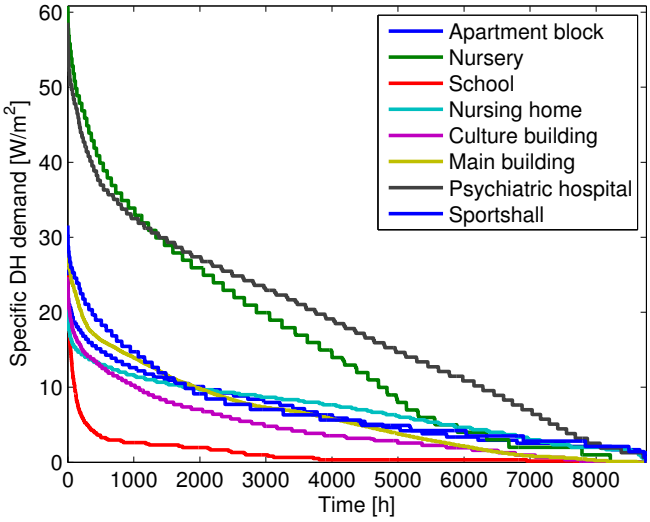

Figure 1: Duration curves for DH demand for the different building types in the modelled neighborhood.

Figure 2 presents the total hourly DH demand for the buildings in Brøset together with the outdoor temperature for 2013. Year 2013 was chosen for the study, as this year had on average normal temperature levels, seen from a statistical perspective. This year was characterized by very low temperatures during the first months of the year, reflected in a high peak DH demand (4800 kW). The load characteristic of the area can be described by the coincidence factor S, defined as

$$S = \frac{P_{max,tot}}{\sum_i P_{max,i}} \tag{1}$$

where $P_{max,tot}$ is the maximum total load for all the buildings in the area, and $P_{max,i}$ is the maximum load for an individual building. The coincidence factor was 0.93 for the modelled building stock based on real DH use data. This indicates a very high simultaneity for the peak heating demands, resulting from a high share of apartment buildings with similar load profiles.

2.2. Modelling approach

The modelling was done using the dynamic simulation program Dymola, version 2017, utilizing a component oriented physical modelling approach supported by the Modelica modelling language [14] and the TIL thermal component library [15]. With this approach, all the created components, such as pipes and buildings, represent real physical parts in the system, and can be re-used in different settings. Both text-based and graphical user interfaces are included in Dymola.

Being a dynamic simulation program implies that the simulated variables are obtained as a function of time for each component. Variables do not need to have explicit expressions; the Modelica code is transformed into efficient simulation code by Dymola using symbolic manipulation. Several numerical solvers are included in Dymola and the standard solver, DASSL, was used for this study.

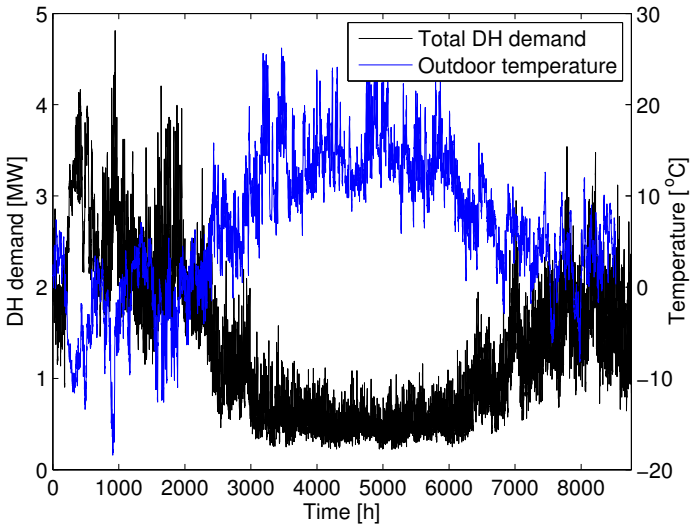

Figure 2: The total hourly DH demand for the buildings in Brøset and ambient temperature in Trondheim in 2013.

The modelled network included the building stock, pipe network, and a heat supply plant delivering heat at the desired temperature level and the required pressure. These components are described in more detail below, and an outline of the network model in Dymola is shown in Figure 3. The chosen modelling approach ensured that the time delay between the different grid elements, as well as the mixing of flow from different return lines with different temperature was included in the system model. This allowed the thermal storage capacity of the network to be simulated realistically. It further allowed realistic regulation using PI-controller blocks, which led to the controlled variables to deviate slightly from the set-point values.

2.2.1. Building models

In the modelled network, the building models represent the customer substations. The model was simplified such that subareas consisting of several buildings of the same type were modelled as single large buildings. Each building model (substation) controls its mass flow rate and heat supply from the heat grid based on the DH demand taken as input and the DH supply temperature, which is continuously measured. The mass flow rate is controlled by a valve coupled to a PI-controller. The heat exchange takes place in a simple pipe model with a heat transfer rate based on the DH demand data.

This approach was chosen because the objective was to study the effects of lower distribution temperatures on the primary side, that is, as seen from the perspective of the DH supplier. The effects on the secondary side were not of interest in this study, and were not modelled. This resulted in a more simple model and thereby faster simulations, and no assumptions considering the temperature levels or control of space heating and DHW preparation at the customers were needed. The approach did however make the return temperatures more equal for the different buildings than if heat exchangers had been used, and also made the return temperature a function of inlet temperature alone, i.e., independent of mass flow.

2.2.2. The network

The pipe models forming the network included hydraulic and heat losses. This section presents the approach taken for modelling these losses, as well as for dimensioning the pipes.

Pressure loss and dimensioning of the pipes. To model the hydraulic losses in the pipe, an approach similar to [16] was adopted. The pressure drop was calculated using the basic equation for fluid inside a circular channel, i.e. the

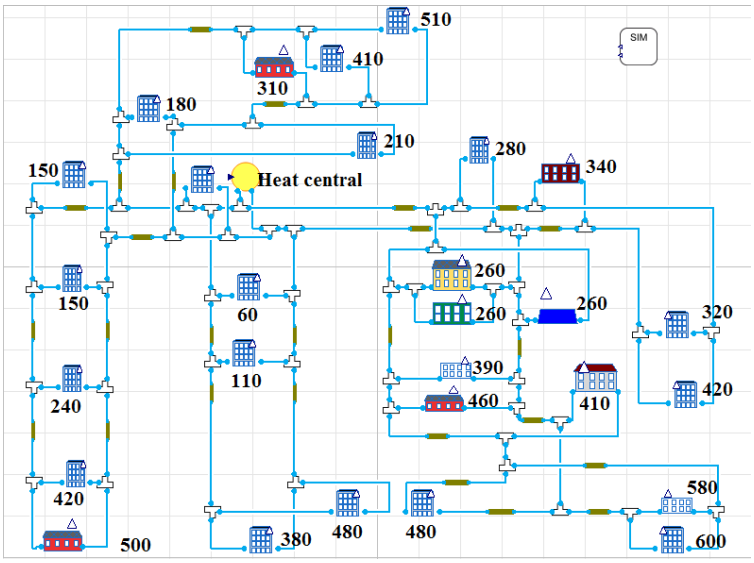

Figure 3: The modelled building area in Dymola, including different building types and a heat supply plant. Approximate distances from the heat supply plant are given in meters. The building closest to the heat supply plant was co-located with the plant. The brown segments represent the pipe models.

Darcy-Weisbach equation [17]:

$$\Delta p = f \cdot \frac{\rho v^2}{2D} L = f \cdot \frac{8\dot{m}^2}{\pi^2 D^5 \rho} L = R \cdot L \tag{2}$$

Where D is the pipe diameter, L the length of the pipe segment, ρ the water density, v the flow velocity, and f is the friction factor. The piping distances were approximated using the building plan, as shown in Figure 3. For the friction factor, the following expression was used, assuming smooth pipes [18]:

$$\frac{1}{\sqrt{f}} = -2.0 \log_{10}\left(\frac{2.51}{\sqrt{f} Re}\right) \tag{3}$$

The friction factor was assumed to be constant in the simulations, however Eq. (3) was needed for finding an expression for pipe diameter as a function of maximum mass flow (see below). The maximum pressure drop per unit length was set to $R = \Delta p / L = 150$ Pa/m.

The pipes in the heating grid were dimensioned based on the maximum mass flow for each segment. An expression for the diameter as a function of maximum mass flow was hence needed. This was done as follows:

1. Choose an arbitrary mass flow rate in relevant range
2. Assume maximum pressure drop, $\Delta p / L = 150$ Pa/m
3. Estimate the diameter such that Eqs. (2) and (3) are valid

Using this procedure, the pipe diameter was calculated for different values of mass flow rate. Thereafter, an empirical equation for the diameter as a function of maximum mass flow rate, $\dot{m}_{max}$, was obtained by least squares fitting, as shown in Figure 4. The resulting equation was

$$D = 0.0379 \cdot \dot{m}_{max}^{0.37}. \tag{4}$$

Once the expression for diameter as a function of mass flow rate had been obtained, the pipe diameters for each segment could be easily calculated. The maximum mass flow is determined by the (maximum) heat demand and the corresponding supply and return temperatures, while the pipe diameter has a negligible effect on the mass flow. This was verified by simulations. The values for $\dot{m}_{max}$ could thus be found by running a simulation for one year assuming uniform pipe diameters. Based on the obtained values for $\dot{m}_{max}$, ideal diameters were calculated using Eq. 4. Realistic pipe diameters were then chosen based on values from [19], always rounding up such that $R \leq 150$ Pa/m was fulfilled for each pipe. The pipe model was discretizised in three pipe cells in the direction of the flow.

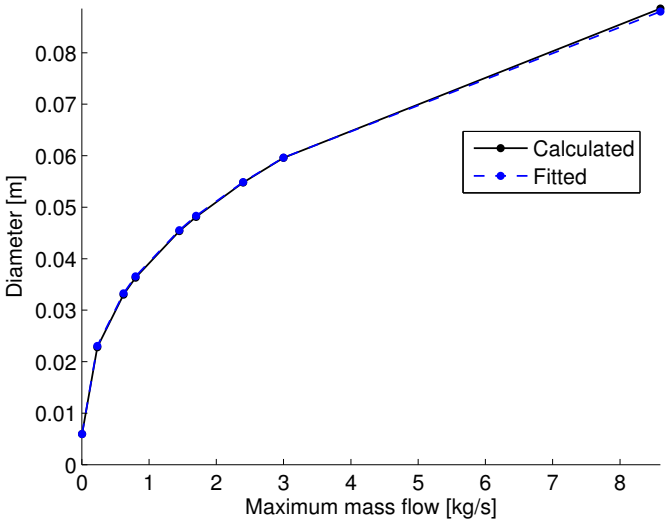

Figure 4: Pipe diameter as a function of maximum mass flow: calculated assuming maximum pressure drop and using Eqs. (2) and (3), and fitted using Eq. (4).

Heat loss. In the present model, the supply and return lines were modelled as two separate pipes buried underground. Conduction heat transfer was found to be the dominating heat loss mechanism, with thickness and thermal conductivity of the insulation as the determining factors. Convection heat transfer from the water to the pipe surface as well as the conduction through the pipe wall were included first, however these found to have negligible effect. This was also concluded in [20]. Convection heat transfer was additionally computationally heavy to calculate. The heat loss could therefore be calculated as:

$$\dot{Q}_{loss} = \frac{2L\pi\lambda_{ins}\left(T_{water} - T_{ground}\right)}{\ln\left(\frac{2s_{ins}+D}{D}\right)} \tag{5}$$

where λ_{ins} is the thermal conductivity, set to 0.022 W/(mK) [19], and s_{ins} is the insulation thickness. Values for s_{ins}, corresponding to the pipe diameter, were similarly found from [19]. The ground temperature T_{ground} was assumed to be constant (5 °C) in the calculations. A more complex heat loss model, including the effect of varying ground temperature and a temperature dependent thermal conductivity is discussed in Section 4.

As the supply and return lines are often placed together, heat can leak from the supply to the return line. This increases the heat losses in the supply line, yet reducing the overall losses as part of the heat lost from the supply line is transferred to the return line. The thermal interaction between the supply and return lines decreases with increasing distance between the pipes. In the present study, this distance was assumed to be large enough (> 20 cm [21]), such that the thermal interaction between supply and return pipes could be neglected.

2.2.3. Heat supply plant

The heat supply plant ensures that heat at the desired supply temperature level and the required pressure difference and mass flow rate is delivered, depending on the outdoor temperature. The heat supply plant contains a circulation pump with a constant efficiency of 40 %, and the pump is controlled by a PI-controller to achieve the required pressure lift. Having a pump with an efficiency dependent on mass flow was tested, however this made the simulations slower, and the effect on the total pump energy was small. An efficiency of 40 % is somewhat lower than the average efficiency of new commercial pumps, but should correspond to an average efficiency of existing, older pumps. To be able to supply heat to the entire network, the PI-controller for the pump requires the signal of the lowest pressure difference in the system, corresponding to the building furthest away, as an input. The minimum pressure difference in the system was set to 70 kPa, as this is the value guaranteed by the local DH supplier in Trondheim. Customers located close to the central receive a much higher pressure difference than this, and this extra pressure is handled by the control valve.

Table 2: The different simulated scenarios and their supply (T_{supply}) and return (T_{return}) temperatures.

Case	T_{supply} [°C]	T_{return} [°C]	Comments
95	95-70	47.5-35.0	–
65	65	32.5	–
55	55	27.5	–
55P	55	27.5	Pipe diameters 50 % larger
LR	95-70	40.5-28.0	Lowered return temp. (by 7 °C)
PS	95-70	47.5-35.0	Peak shaving (max. demands reduced by 20 %)

2.3. Simulations

Three supply temperature levels were considered: 95, 65 and 55 °C. 95 °C represents the current practice, whereas 65 °C is considered as a potential future temperature level, considering the Norwegian legislation; and 55 °C was investigated as this represents an ultimate goal for the LTDH systems. For the highest temperature level, the supply temperature was outdoor temperature compensated according to the present practice of the local DH operator: assuming a supply temperature of 95 °C at outdoor temperatures of -20 °C and lower, and a temperature of 70 °C at +15 °C and higher, and a linear decrease in between the two limits. For 65 and 55 °C, constant supply temperatures were applied throughout the year.

To be able to calculate the mass flow set-point for each building, the desired return temperature level had to be defined. According to the local DH provider, existing networks in Denmark have supply/return temperature limits of approximately 90/45 °C and 50/25 °C. The required mass flow was calculated using these limits for return temperature, and assuming a linear relationship between them. A valve controlled the mass flow to achieve the desired return temperature, given the known heat demand and inlet temperature. As the controller is not perfect, the actual, regulated mass flow resulted in some deviations from the targeted values in the return temperature.

For the high-temperature case, a scenario assuming return temperatures 7 K lower than the given limits was additionally included in order to study how lower return temperature affects the circulation pump energy, and the heat losses. The different simulated scenarios are shown in Table 2.

Lower supply temperature will result in a lower temperature drop at the customer, and thereby a higher mass flow rate is needed to cover the heat demand. This will increase the pressure drop in the pipes beyond the allowable limit of 150 Pa/m and accordingly the pump power. Therefore, for the case with a supply temperature of 55 °C, a case assuming 50 % bigger pipe diameters was simulated as well, yielding a total pump power similar to that of the 95 °C case.

Peak shaving is a relevant measure to reduce the required installed heat capacity and the demand for peak heating devices, which often operate with fossil fuels, having high operation costs and a negative environmental impact. In practice, this can be implemented by using thermal storage, such as hot water tanks, together with intelligent control systems to predict peak heating periods and divide the load over the preceding hours [10]. In our model, peak shaving was implemented in the input heat demand data for each building type such that heating demands exceeding 80 % of the annual peak heating demand were distributed to five hours preceding the high-demand period. This measure had however hardly any impact on the total heat losses or the pump energy, and peak shaving was hence implemented only for the highest supply temperature case. No thermal losses from the thermal storages were accounted for, as the aim was only to estimate the potential savings while avoiding excessive computation times.

2.4. Energy mix and GHG emissions

An important aspect in shifting to lower distribution temperatures is the increased possibility for utilization of renewable and waste heat sources, and hence reduction in the GHG emissions related to DH. Although alternative heat sources were not included in the model at this stage, calculation of the GHG emissions was included, based on the actual energy mix applied by the local DH provider. The heat production is divided between the different sources, depending on the heat demand. For low demands, a large central boiler operating on municipal solid waste (MSW) is the only heat source. For higher heat demands, peak heating devices, such as heat pumps and biomass, electric and oil

Table 3: The energy mix considered, including the operating limits of the different sources (minimum and maximum heat demand to employ the source), and the equivalent CO_2 emissions per kWh heat produced. The maximum limit for the oil boiler was not known.

Heat source	Operation limits [kW] Lower	Upper	Emissions [g CO_2-eqv./kWh]
Waste (MSW)	0	1671	11.2
Bio-boiler	1671	1805	19.8
Biogas	1805	1823	39.6
Heat pump	1823	1853	36.7
Electricity	1853	2133	110.0
LNG	2133	2173	243.0
LPG	2173	3072	274.0
Oil	3072	–	292.0

boilers, are added such that the least polluting sources are used first. The considered heat sources are given in Table 3. The table presents the operating limits of the different sources (minimum and maximum heat demand to employ the source), as well as the associated equivalent CO_2 emissions per kWh heat produced.

In the model it was assumed that the high-temperature (95-70 °C) case would have the same total energy mix over one year as the one from the local DH supplier. The capacity limits for each heat source were set so that this assumption was valid, and these limits were assumed also to the other supply temperature levels. Each source was assumed to be able to supply a constant, limited amount of heat. Hence, the difference in equivalent CO_2 emissions for the different scenarios was based on the differences in the heat demand as seen from the heat supply plant.

3. Results

Table 4 shows the results from a simulation over one year for the different scenarios given in Table 2. Included in Table 4 are results for the total and maximum heat delivered, heat losses, and pump energy and power demand; supply pressure and mass flow; as well as the global warming potential (GWP). Both the absolute value and the relative value as compared to the baseline case with 95-70 °C supply temperature are given.

Table 4: Simulation results over one year for the different cases: The total annual heat delivered (Q_{tot}), heat losses (Q_{loss}) and pump energy (W); maximum heat delivered (P_{max}) and pump power ($\dot{W}_{max}$); maximum and average mass flow ($\dot{m}_{max}$ and $\dot{m}_{ave}$); maximum and average supply pressure ($p_{supply,max}$ and $p_{supply,ave}$); and the GWP as total CO_2 emission equivalents. The results are given as the total amount over a year, and as a percentage compared to the baseline case (95).

Case name/ Variable	95		65		55		55P		LR		PS	
	Tot.	%	Tot.	%	Tot.	%	Tot.	%	Tot.	%	Tot.	%
Q_{tot} [GWh]	11.9	100	11.8	99.3	11.7	98.6	11.8	99.0	11.8	99.7	11.9	100
Q_{loss} [MWh]	494	100	414	83.6	342	69.2	381	76.8	450	90.8	494	100
W [MWh]	23.3	100	35.0	150	48.6	209	23.3	100	15.7	67.3	23.2	99.9
P_{max} [MW]	4.6	100	4.6	99.9	4.6	99.5	4.6	100	4.6	100	4.1	88.1
$\dot{W}_{max}$ [kW]	19.7	100	44.0	223	66.5	337	19.5	98.9	11.6	58.8	16.5	83.6
$\dot{m}_{max}$ [kg/s]	25.5	100	34.7	134	40.3	158	40.3	158	20.6	80.7	23.5	92.2
$\dot{m}_{ave}$ [kg/s]	8.9	100	10.7	120	12.4	139	12.4	140	7.2	80.3	8.9	100
$p_{supply,max}$ [bar]	4.1	100	6.1	149	7.6	187	2.9	72.2	3.2	79.7	3.8	93.5
$p_{supply,ave}$ [bar]	2.1	100	2.3	110	2.5	120	1.9	88.7	2.0	93.2	2.1	100
GWP [tons CO_2-eqv.]	432	100	423	98.0	418	96.8	421	97.5	428	99.2	432	100

Results of the most interest are the heat losses and the pump energy use (W). Figure 5 presents these results for each case with respect to the total heat delivered (Q_{tot}), Q_{loss}/Q_{tot} and W/Q_{tot}, as an indication of the global energy efficiency. As the pump energy was an order of magnitude lower than the heat losses, W/Q_{tot} was multiplied by ten. In addition, the ratio between the total pump energy use and heat losses is included in Figure 5.

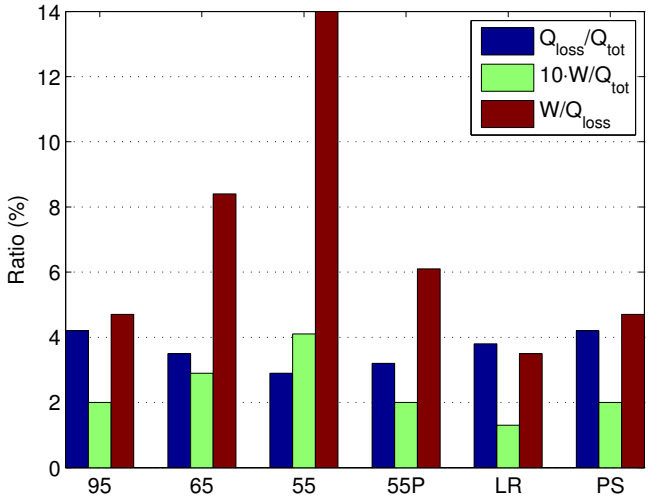

Figure 5: The ratio between the total annual heat losses and the total heat delivered, the pump energy use and the total heat delivered multiplied by ten, as well as between the pump energy use and the heat losses.

For the 55 case, the relative heat losses are 31 % lower (2.9 %) than for the 95 case (4.2 %). The heat losses are generally low, largely owing to the small size of the heat grid: the total length of the pipeline was only 3.55 km. The linear heat demand density for the area was 3.2 MWh/year per grid meter. Furthermore, the annual average supply temperature for the 95 case was relatively low, 76 °C, due to a relatively mild winter and a long period during the summer with a nearly constant supply temperature of 70 °C. The obtained heat loss per meter grid (trench) was 16 W for the 95 case, while normal values are 10-30 W/m for the somewhat higher supply temperatures usually applied. The heat losses were thereby realistic and the applied heat loss model could be considered reliable.

The relative pump energy use for the 55 case was 0.41 %, which is 109 % higher than for the 95 case (0.20 %). The pump energy use is however an order of magnitude lower than the heat losses. In Figure 5, the ratio between the total pump energy and the total heat delivered is therefore scaled up by a factor of 10. The total pump energy use was the lowest, 0.31 % of the total heat delivered, for the low return case. This was expectable, since the heat demand was the same, but temperature difference at the customers is higher, yielding a lower mass flow rate.

Figure 6 shows the total pump energy use plotted over the total heat loss for the different cases. For the 55P case with 50 % larger pipe diameter, the total pump energy was almost identical with the 95 case, as intended. The heat loss is 23 % lower for the 55P case compared to the 95 case. Based on Figure 6, the 55P case appears as the most optimal solution with respect to heat losses and pump energy demand.

The peak shaving case is almost similar with the 95 case in terms of total heat losses and pump energy; the difference becomes only visible in the maximum heat delivered and pump power (12 and 16 % lower than the baseline case, respectively; see Table 4). Peak shaving measures are hence most important in enabling reduced installed capacity. The fact that the reduction in the total maximum heat delivered was lower than the 20 % peak reduction applied for the individual buildings is probably because the peak demands of the different building types do not occur simultaneously. It is also worth mentioning that for the simulated year, the coldest day of the year was clearly colder than the rest of the year (see Figure 2). This lead to a high peak heating demand with respect to the average demand, and lowered the effect of peak shaving. The utilization time for the year was 2206 h, and the load factor was 0.25, which is considered to be low [22]. To obtain a bigger impact, another peak shaving approach, or simply a lower threshold for the peak shaving, could be applied.

The low return case gave the lowest mass flow rate and total pump energy, as expected. The reductions were quite large, around 20 % reduction in both maximum and average mass flow rate and 33 % in total pump energy with respect to the baseline case. Peak pumping power was 41 % lower. Furthermore, the heat losses were reduced by 9 % due to lower mass flow rates and return temperatures.

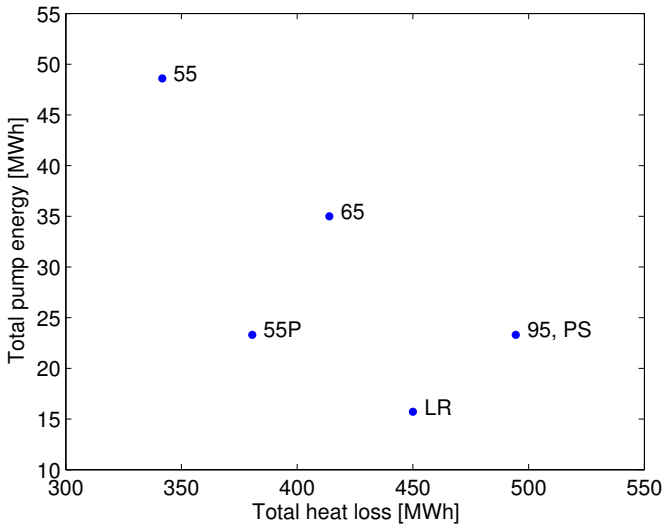

Figure 6: Total pump energy plotted over the total heat loss for the different cases.

Figure 7 presents the pressure lift as a function of mass flow rate at the heat supply plant. In Figure 7, the coldest winter day is visible as a distinct peak in the mass flow rate vs. pressure lift for all other cases apart from peak shaving, which does not have this peak. The 55P case with bigger pipe diameters, shows more moderate increase in pressure lift with respect to the other cases, in accordance with Eq. (2). The low return case shows lowest mass flow rate and pressure lift, which is in line with the low pump energy use as discussed earlier.

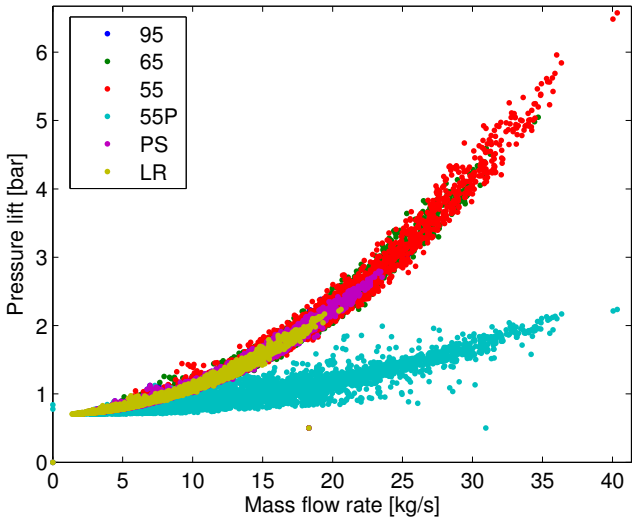

Figure 7: Pressure lift required by the pump as a function of mass flow rate in the heat supply plant.

Figure 8 presents the mass flow rate as a function of ambient temperature for the different simulated scenarios. At ambient temperatures (T_{amb}) above approximately 18 °C, the mass flow rate is almost independent of T_{amb} and relatively similar for the different cases. This is most probably because at these temperature levels, the heating demand is primarily due to DHW preparation. At lower temperatures, strong dependency on T_{amb} and great variation

between the simulated cases is present. At 5 °C ambient temperature for instance, the lowest mass flow rates, obtained for the LR case, are around 5 kg/s; while for 55 and 55P cases, mass flow rates up to 35 kg/s are observed.

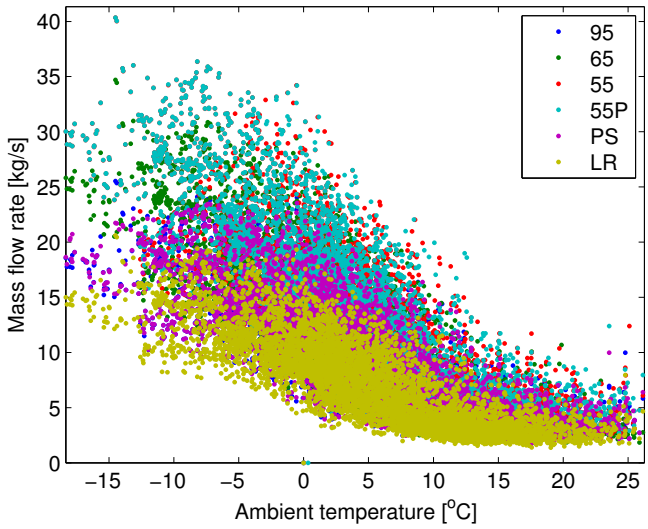

Figure 8: Mass flow rate as a function of ambient temperature for the different simulated scenarios.

4. Discussions

4.1. Heat losses

Lower heat losses is one of the primary motivations for shifting to LTDH. In the present study, the heat losses were 31 % lower for the 55 case (constant supply temperature of 55 °C) as compared to the reference case with a supply temperature of 95-70 °C. In a similar simulation case study carried out for Graz, Austria [5], a reduction in heat losses of 29 % was obtained comparing a reference scenario with a supply temperature of 120-75 °C to a LTDH scenario with a constant supply temperature of 58 °C. In another case study carried out for a network with low linear heat demand densities in Denmark, the heat losses were almost halved when comparing a baseline scenario (supply temperature 85 °C all year round) with a LTDH scenario (supply temperature 55 °C for normal conditions and optimal design to allow low return temperatures). Hence, the reduction in heat losses obtained in the present study appears reasonable.

Overall, the heat losses were very low in the present study: 4 % for the highest supply temperature case, and 3 % for the lowest supply temperature case. The present DH system in Trondheim (covering the whole city) has heat losses of approximately 10-12 %. This deviation can however be attributed to the particularly high linear heat demand density for the studied case; heat losses per meter trench were realistic when comparing to the existing network, as discussed in Section 3. The high linear heat demand density is probably partially due to the fact that subareas of several similar buildings were modelled as single large buildings, as explained in Section 2.2.1. The reduction in grid length resulting from this simplification will be taken into account in a further study.

Comparison of the applied heat loss model to a more complex model was also performed using a simple network with only two buildings and a heat supply plant providing water at 95-70 °C over a distance of 100 m. The more complex pipe models had ten pipe cells along the pipe; varying ground temperature over the year (sinusoidal variation by ±4 K as in [20]; temperature dependent insulation conductivity according to [23]); and a radially sectioned insulation and surrounding ground layer (four layers each). For the insulation, both temperature and conductivity were varied from layer to layer; for the ground, only the temperature was varied, and for the conductivity, a constant value of 1.6 W/(mK) was assumed [20]. The uncertainty of soil conductivity is generally high – values between 0.5-2.5 W/(mK) have been reported, depending on the soil type and moisture content [20].

With the more advanced heat loss model, 9 % lower total annual heat losses were obtained. From the studied parameters, variation in ground temperature hardly affected the results, while the insulation conductivity was of major importance. The level of complexity was however strongly increased, although the simulation time was hardly affected in the tested simple network. In a future model, a more complex heat loss model may be applied.

4.2. GHG emissions

The heating demand of the buildings in the network was identical for each simulated case. The reduction in the delivered heating – and in the GHG emissions – was hence solely due to reduction in the heat losses. The relative reduction in heat losses and emissions is however not similar for the different cases (see Table 4). In periods with high heating demand, when the heat demand is reduced due to the lower loss at lower supply temperatures, the heat sources to be removed are always the most polluting ones. Therefore, a stronger reduction in the GHG emissions with respect to the heat supply should be expected. For the PS case, the GHG emissions were not reduced despite a 12 % lower peak demand compared to the 95 case. The reason for this is probably the low load factor as discussed earlier; most of the year the heat demand is identical for the PS and 95 cases. For all the other cases, the relative reductions in emissions are higher than the reductions in heat losses, and hence in the energy demand. The lowest GHG emissions were obtained for the 55 case, with 3 % reduction in emissions as compared to the reference case. Obviously, the full potential of LTDH in terms of reduced GHG emissions is only seen when the heat supply is based on renewable and waste heat resources.

4.3. Pipe dimensions

According to [23], the DH network should be designed according to the maximum hydraulic load that can be withstood by the distribution pipeline (pressures of 1.2-1.5 times the nominal value). The duration of peak load, when the maximum pressures might occur, is marginal, and hence it is recommended to utilize the maximum pressure that can be withstood by the DH pipes in order to reduce pipe diameters and consequently decrease the heat losses in the network [23]. Based on the simulation results however, the 55P case appears as the most optimal solution with respect to both the heat losses and pump energy demand, as discussed in Section 3. Nevertheless, the pipe diameter, together with the insulation thickness and temperature levels, is a decisive factor in determining the heat losses and hence the cost-effectiveness of the DH system [24]. Alternative approaches for dimensioning the pipes, such as those suggested in [24], could be considered in further studies for finding the most optimal pipe diameters.

5. Conclusions

In this study, a heating network for a residential area in Trondheim, Norway, has been modelled using the dynamic simulation program Dymola in order to investigate the benefits of LTDH. Heat losses, pump energy use and GHG emissions were analyzed for six different cases, including three different supply temperature levels: 95-70 °C with outdoor temperature compensation, and constant supply temperatures of 65 and 55 °C. A scenario assuming bigger pipe diameters was also included for the 55 °C case. In addition, the effect of peak shaving and lower return temperature levels were studied for the highest supply temperature case.

The simulation results showed that reducing the supply temperature has a significant impact on the heat losses. By lowering the supply temperature to 55 °C, the heat losses could be reduced by approximately one third. The heat losses obtained were generally low: only 4 % of the total delivered heat for the reference case supplying heat at 95-70 °C, owing to the high heat demand density of the network, and a mild year, yielding low average supply temperatures.

The total pump energy demand was doubled for the 55 °C supply temperature case as opposed to the reference case; however, the total pump energy was generally an order of magnitude lower than the heat losses. Hence, reducing the supply temperature has a positive overall environmental impact. With bigger pipe dimensions, the pump energy demand for the low-temperature case could be kept at the same level as in the high-temperature case, while the heat losses were still reduced significantly. Lowering the return temperature in the high-temperature case showed also to be very beneficial in reducing both pump work and heat losses. Peak shaving did not have any impact on the total heat losses or the pump power, but reduced the peak heating demand and the pump power significantly. Furthermore, with lower heat losses resulting from lower supply and return temperatures, lower GHG emissions were obtained, as the use of peak heating devices based on fossil fuels or electricity could be reduced.

Future work will encompass including different renewable and waste heat sources as well as thermal storage into the model. Furthermore, an approach for calculating the total costs will be included, to be able to fully compare the different scenarios.

Acknowledgements

This work has been carried out as a part of the project Development of Smart Thermal Grids, supported by the Research Council of Norway (RCN) under grant agreement number 245355, and Statkraft Varme AS. The authors would like to specifically thank Åmund Utne from Statkraft Varme AS for providing information regarding the DH network in Trondheim.

References

[1] D. Connolly, H. Lund, B. V. Mathiesen, S. Werner, B. Möller, U. Persson, T. Boermans, D. Trier, P. A. Østergaard, S. Nielsen, Heat Roadmap Europe: Combining district heating with heat savings to decarbonise the EU energy system, Energy Policy 65 (2014) 475–489.

[2] H. Lund, S. Werner, R. Wiltshire, S. Svendsen, J. E. Thorsen, F. Hvelplund, B. V. Mathiesen, 4th Generation District Heating (4GDH): Integrating smart thermal grids into future sustainable energy systems, Energy 68 (2014) 1–11.

[3] T. Ommen, W. B. Markussen, B. Elmegaard, Lowering district heating temperatures - Impact to system performance in current and future Danish energy scenarios, Energy 94 (2016) 273–291.

[4] A. Dalla Rosa, J. E. Christensen, Low-energy district heating in energy-efficient building areas, Energy 36 (12) (2011) 6890–6899.

[5] M. Köfinger, D. Basciotti, R. Schmidt, E. Meissner, C. Doczekal, A. Giovannini, Low temperature district heating in Austria: Energetic, ecologic and economic comparison of four case studies, Energy 110 (2016) 95–104.

[6] P. K. Olsen, C. H. Christiansen, M. Hofmeister, S. Svendsen, J.-E. Thorsen, O. Gudmundsson, M. Brand, Guidelines for low-temperature district heating, EUDP 2010-II: Full-Scale Demonstration of Low-Temperature District Heating in Existing Buildings (2014).

[7] Direktoratet for Byggkvalitet, Byggteknisk forskrift (TEK 10): Veiledning om tekniske krav til byggverk (2011).

[8] L. Giraud, R. Baviére, M. Vallée, C. Paulus, Presentation, validation and application of the districtheating modelica library, in: Proceedings of the 11th International Modelica Conference, Linköping University Electronic Press, 2015.

[9] D. Olsthoorn, F. Haghighat, P. A. Mirzaei, Integration of storage and renewable energy into district heating systems: A review of modelling and optimization, Solar Energy 136 (2016) 49–64.

[10] D. Basciotti, R. Schmidt, Peak reduction in district heating networks: a comparison study and practical considerations, in: The 14th International Symposium on District Heating and Cooling, 2014.

[11] F. Soons, J. I. Torrens, J. Hensen, R. D. Schrevel, A modelica based computational model for evaluating a renewable district heating system, in: 9th International Conference on System Simulation in Buildings, 2014.

[12] H. Kauko, Heating and cooling demand of buildings in trondheim a pre-study for designing local low-temperature thermal grids, Project report for Development of Smart Thermal Grids (DSTG), RCN grant no 245355 (2015).

[13] S. Norge, Kriterier for passivhus og lavenergibygninger - boligbygninger (2013).

[14] Modelon, Dymola (2015).
URL http://www.modelon.com/products/dymola/

[15] TLK-Thermo, TIL Suite - Simulates thermal systems (2016).
URL https://www.tlk-thermo.com/index.php/en/software-products/til-suite

[16] P. Li, N. Nord, I. S. Ertesvåg, Z. Ge, Z. Yang, Y. Yang, Integrated multiscale simulation of combined heat and power based district heating system, Energy Conversion and Management 106 (2015) 337–354.

[17] S. Frederiksen, S. Werner, District heating and cooling, Studentlitteratur AB, 2014.

[18] F. P. Incropera, D. P. Dewitt, T. L. Bergman, A. S. Lavine, Principles of Heat and Mass transfer, Wiley, 2013.

[19] LOGSTOR (2016).
URL https://www.logstor.com/

[20] A. Dalla Rosa, H. Li, S. Svendsen, Method for optimal design of pipes for low-energy district heating, with focus on heat losses, Energy 36 (5) (2011) 2407–2418.

[21] E. K. L. Nielsen, Lavtemperatur-varmenett, Project Thesis, Norwegian University of Science and Technology (NTNU) (2016).

[22] T. Tereshchenko, N. Nord, Implementation of CCPP for energy supply of future building stock, Applied Energy 155 (2015) 753–765.

[23] C. Christiansen, O. Paulsen, B. Bøhm, J. Thorse, C. T. Larsen, B. Jepsen, P. Olsen, H. Lambertsen, R. Hummelshøj, S. Svendsen, Udvikling og demonstration af lavenergi-fjernvarme til lavenergibyggeri, Hovedrapport og bilag, Teknologisk Institut, Taastrup, Denmark (2009).

[24] H. I. Tol, S. Svendsen, Improving the dimensioning of piping networks and network layouts in low-energy district heating systems connected to low-energy buildings: A case study in Roskilde, Denmark, Energy 38 (1) (2012) 276–290.